AIChE

Modeling Dynamic Functioning of Rectangular Photobioreactors in Solar Conditions

J. Pruvost
GEPEA, Université de Nantes, CNRS, UMR6144, bd de l'Université, CRTT - BP 406, 44602 Saint-Nazaire Cedex, France

J. F. Cornet
Clermont Université, ENSCCF, EA 3866 - Laboratoire de Génie Chimique et Biochimique, BP 10448, F-63000 Clermont-Ferrand, France

V. Goetz
PROMES-CNRS, UPR 8521, Tecnosud, Rambla de la Thermodynamique, 66100 Perpignan, France

J. Legrand
GEPEA, Université de Nantes, CNRS, UMR6144, bd de l'Université, CRTT - BP 406, 44602 Saint-Nazaire Cedex, France

DOI 10.1002/aic.12389
Published online September 7, 2010 in Wiley Online Library (wileyonlinelibrary.com).

A generic model for the simulation of solar rectangular photobioreactors (PBR) is presented. It combines the determination of the time-varying solar radiation intercepted by the process with the theoretical framework necessary for PBR simulation, namely modeling of the radiant light energy transport inside the culture volume, and its local coupling to photosynthetic growth. Here, the model is applied to illustrate the full dependency of PBR behavior on solar illumination regimes, which results in a complex, transient response. Effects of day–night cycles, culture harvesting, and the interdependency of physical (light) and biological (growth) kinetics are discussed. It is shown that PBR productivity is the result not only of light intercepted on the illuminated surface but also of light attenuation conditions inside the bulk culture as influenced by incident angle and beam/diffuse distribution of solar radiation. Results are presented for a location in France for 2 months representative of summer and winter.
 AIChE J, 57: 1947–1960, 2011
Keywords: photobioreactor, solar, modeling, microalgae, radiative transfer

Introduction

Photosynthetic microorganisms (microalgae and cyanobacteria) allow higher areal productivities than plants, and so are often put forward as one of the more promising primary resources in domains including feedstock (proteins and lipids) and biofuel production, with various energy vectors such as H_2, lipids for biodiesel fuel, sugar for gasification, or fermentation.[1–6] However, their production requires the design and optimization of specific cultivation systems. Unlike heterotrophic microorganisms such as yeasts and bacteria, for which the classical stirred vessel is widely used at the industrial scale, cultivation systems for photosynthetic microorganisms are wide ranging. This diversity is explained mainly by a well-known limitation, which is the capacity of these systems to transfer photons within the bulk culture to ensure photosynthetic growth. The main consequence of the high light energy demand is that cultivation systems for

Correspondence concerning this article should be addressed to J. Pruvost at jeremy.pruvost@univ-nantes.fr.

photosynthetic microorganisms have to present high illuminated areas relative to the volume of the bulk culture, where light attenuation occurs. This and other constraints, especially the need for mixing to ensure culture homogeneity, explain the variety of geometries met, from open ponds to closed optimized photobioreactor (PBR) technology. All have their benefits and limitations, in terms of production scale allowed, construction cost, productivity, control of culture conditions, energy and water consumption, culture confinement, etc. However, whatever the concept, light supply and its use by the culture will always govern the productivity of the cultivation system. As widely reported in the literature,[7–10] this fact results in a significant increase in process complexity, the radiative transfer in turbid media being a physical problem that is difficult to handle and optimize.[11–13]

Cultivation systems for photosynthetic microorganisms can use artificial light or natural sunlight. Obviously, for practical, economic, and environmental reasons, sunlight is to be preferred for mass scale production in extensive systems. However, the wide variability of sunlight in time and space adds further complexity to the optimization and control of the cultivation system, compared with artificial illumination. This explains why most theoretical work has been devoted to artificial light PBRs, where a tight control of the incident light flux is possible. Authors have shown, for example, that certain relevant values, such as PBR productivity and energetic efficiency, can be predicted using a rigorous formulation of radiant light transfer inside the culture and its local kinetic coupling with photosynthetic growth. A theoretical framework developed over many years has proved efficient for various PBR geometries and cultivated species, and for various applications such as biomass and hydrogen production.[14–16] The aim of this work was to extend the knowledge derived from controlled artificial conditions to solar conditions, thereby providing a sound physical basis for subsequent investigation of the specific behavior of solar PBRs.

Compared with other more classical solar processes, PBRs require introducing major specific features. As was confirmed in this study, PBR productivity depends closely on the light collected, as does any light-driven process. However, unlike processes based only on surface conversion, such as photovoltaic panels, solar thermal concentrated conversion or photocatalysis on fixed supports, optimizing the amount of light collected on the PBR surface is not sufficient. Light conversion by photosynthetic microorganisms occurs within the bulk culture. The transfer of the collected light flux inside the bulk culture has thus to be considered for kinetics and energetic formulations. These are not straightforward: they involve specific considerations to determine the irradiance field inside the PBR, which is then coupled with the local kinetics of photosynthetic growth of the cultivated species, so that PBR productivity can finally be simulated. This means first taking into account all aspects influencing radiative transfer inside the turbid medium, namely biomass optical properties and concentration, incident light flux onto the PBR surface defined by the incident angle of the direct radiation and the direct/diffuse radiation proportions as boundary conditions.[11–13,17,18] Second, it is necessary to make a correct formulation of the local and spatial coupling between the radiant volumetric power density absorbed and the kinetic rates and stoichiometries, which are strongly influenced by the radiation field. In outdoor solar PBRs involving different stages and time constants of photosynthesis, this coupling is more complex to manage than for chemical photoreactors,[17,18] although some very basic biomass productivity assessments have been tentatively made in the past from robust knowledge models of light transfer.[13]

The model developed in this work considered all these aspects. It was applied to the particular case of cultivation systems with radiative transfer in Cartesian rectangular geometries, in other words, cultivation systems presenting a flat illuminated surface (such as a flat panel PBR or raceway). The quasi-exact radiative properties (absorption and scattering coefficients, phase function) of the microorganism considered were used at this stage to ensure an accurate description of the radiation field before the kinetic coupling formulation. The study was also restricted to "light-limited" conditions, assuming all other biological needs (nutrients and dissolved carbon) and operating conditions (pH and temperature) were controlled at optimal values. The model was associated with a solar database to facilitate the further investigation of time (day/night and season) and space variability of solar radiation. It was then used to illustrate some significant aspects induced by solar conditions, such as the dynamic regime when operated in day–night cycles, and the role of intercepted light on PBR productivity, as influenced, for example, by season or PBR inclination.

Theoretical Considerations

Light-limited conditions

Because of the high dependency of photosynthetic growth on the light received, it is now well established that PBR performance is highly dependent on light supply. Obviously, the growth of photosynthetic microorganisms is also dependent on various other parameters (pH, temperature, inorganic dissolved carbon, mineral nutrients, etc.). If these parameters are kept at their optimal value, maximal PBR performance can be reached, and PBR productivity for a given species then depends only on the PBR geometry and incident light flux. As discussed and clarified by the authors in recent work, this is the light-limited condition in which light alone limits growth.[19,20] This work was restricted to this specific case but with solar illumination. The assumption of light-limited conditions is a bold one considering the difficulty maintaining optimal growth conditions in large-scale outdoor cultivation systems.[21] However, as PBR productivity is always controlled by the light received, the methodology developed in this work could serve as a theoretical basis for further modeling purposes; other possible adverse effects on biological growth, such as nutrients, dissolved carbon limitation, or nonoptimal temperature, could be integrated later.

PBR geometry simulated

Radiant light energy can be used in two general ways in PBRs: by direct illumination of the cultivation system (surface-lightened PBRs) or by inserting light sources inside the bulk culture (volumetrically lightened PBRs). The second systems allow further optimization of the light use in the

culture by increasing the efficiency of photosynthesis by diluting light, thus leading to higher theoretical surface productivity.[22] They can also be combined with solar-tracking systems, giving an additional possibility of optimization by maximizing light intercepted during the sun's displacement. Although a promising approach, only a few practical realizations have been encountered.[22–26] By contrast, surface-lightened PBRs are more often encountered.[10,21] They have been described with a fixed horizontal position,[27–29] a vertical position,[30–32] and, in a few cases, a tilted position.[33,34] Only surface-lightened PBRs were considered in this study.

Surface-lightened PBRs display a wide variety of geometries, from open ponds to tubular or flat panel PBRs. Depending on the geometries (with respect to the light source position), very different radiation fields can be found in the culture. Our study was restricted to geometries with radiation fields responding to the "one-dimensional" hypothesis, where light attenuation occurs mainly along a single direction perpendicular to the illuminated surface (culture depth). In this case, simple radiative models such as the two-flux model can be applied with relative accuracy (see discussion in the Appendix). Although a more sophisticated method can be used,[11,12] the two-flux model appears to be a convenient compromise, often giving a sufficiently accurate prediction of the radiation field in the context of photosynthetic microorganism cultivation.[20,22,35,36] In the case of the one-dimensional hypothesis, it also provides analytical solutions that facilitate coupling with kinetic growth models, at the same time, reducing the computational effort to simulate, for example, transient conditions as in solar irradiation. This study was thus restricted to PBRs fitting this hypothesis, and more specifically, geometries presenting a flat illuminated surface, corresponding to flat panel geometries, raceways, or open ponds (grouped here under the general term "rectangular PBRs," indicating that they present a Cartesian light attenuation). A rectangular PBR was retained with an arbitrary depth $L_z = 0.1$ m. If needed, the approach could be extended to any other PBR depth and any other PBR geometry, such as tubular or cylindrical ones (with the appropriate radiative transfer model). An example for cylindrical PBR illuminated on one side (a classical configuration encountered in solar production systems) is found, for example, in Loubiere et al.[37] Takache et al.[19] also provides solutions to the two-flux model for various geometries corresponding to the one-dimensional hypothesis. Here, we especially discuss the application of such a model to the solar case, taking into account the variable beam radiation incident angle and the beam and diffuse parts of the solar radiation.

Determination of solar radiation conditions on PBR illuminated surface

The solar energy received on a PBR plane surface is a central characteristic as for any solar process. It is represented by the hemispherical incident light flux density, q, or photon flux density (PFD) as it is commonly named in PBR studies. This allows, for example, to evaluate the ability of a given PBR to collect light as a function of its design, orientation, or inclination. An example is given by Sierra et al.[38] for a flat panel PBR located in southern Spain (Almeria). Influence on light interception of north-south and east-west orientations was investigated for both vertical and horizontal positions. The definition of an optimal orientation of a fixed surface PBR was shown to be nontrivial, depending, for example, on the time of year. This approach was extended here to simulate the resulting biomass growth and PBR productivity. However, further development is needed. Unlike solar processes based on surface conversion (e.g., a photovoltaic panel), determination of global radiation on the PBR surface is insufficient to predict PBR response, as light is converted inside the bulk culture. It is thus necessary to add to PFD determination a rigorous treatment of radiative transfer inside the culture, and then couple the resulting irradiance field with photosynthetic conversion of the algal suspension.

Light penetration inside a turbid medium is affected by the incident polar angle θ of the radiation on the illuminated surface (see Figure 1a and Appendix). For a solar PBR with a fixed position, the earth's rotation makes the incident angle time dependent. By definition, the direction of a beam of radiation that represents direct radiation received from the sun (without scattering) sets the incident polar angle θ on the illuminated surface (Figure 1a) and the direct incident light flux density $q_{//}$. Diffuse radiation corresponds to the solar radiation received after its direction has been changed by scattering through the atmosphere or by reflection from various surfaces, such as the ground, "seen" by the interception surface (Figure 1b). Diffuse radiation cannot thus be defined by a single incident angle but instead has an angular distribution on the illuminated surface (on a 2π solid angle for a plane).

This diffuse radiation and its angular distribution on a surface is affected by the sun's position in the sky, by meteorological conditions, by ground albedo (grass, sand, snow, etc.), by nearby buildings, etc., and so exact determination requires complex models, named "sky models." For the sake of simplicity, the Perez model[39] was retained in this study. Like many other models, it allows only total diffuse radiation on the surface to be calculated, thus assuming an isotropic angular distribution on the 2π solid angle (on a flat surface). This is a usual assumption in solar processes and so it was retained here.[40] However, for PBR applications, it would be of interest in future studies to improve this representation because of the dependency of radiative transfer inside the bulk culture on the angularity of incident diffuse PFD.

The earth's sphericity, its rotation, and variable atmospheric conditions make solar radiation at the earth's surface very complex, with high variability in time and space. Determination of light intercepted for a given PBR location on earth will be a function of its geometry, inclination (relative to the ground), and orientation (north-south). Mathematical relations are available to determine radiation conditions on a collecting surface as a function of all these conditions. An example was recently given by Sierra et al.[38] for solar PBRs. A full description of the mathematical relation can also be found in Duffie and Beckman.[40] Some commercial software integrating solar models are also available. They allow typical day evolution of irradiation on a given surface to be easily generated (as characterized by its inclination and orientation), for almost any earth location and time of year. We opted for this approach here.

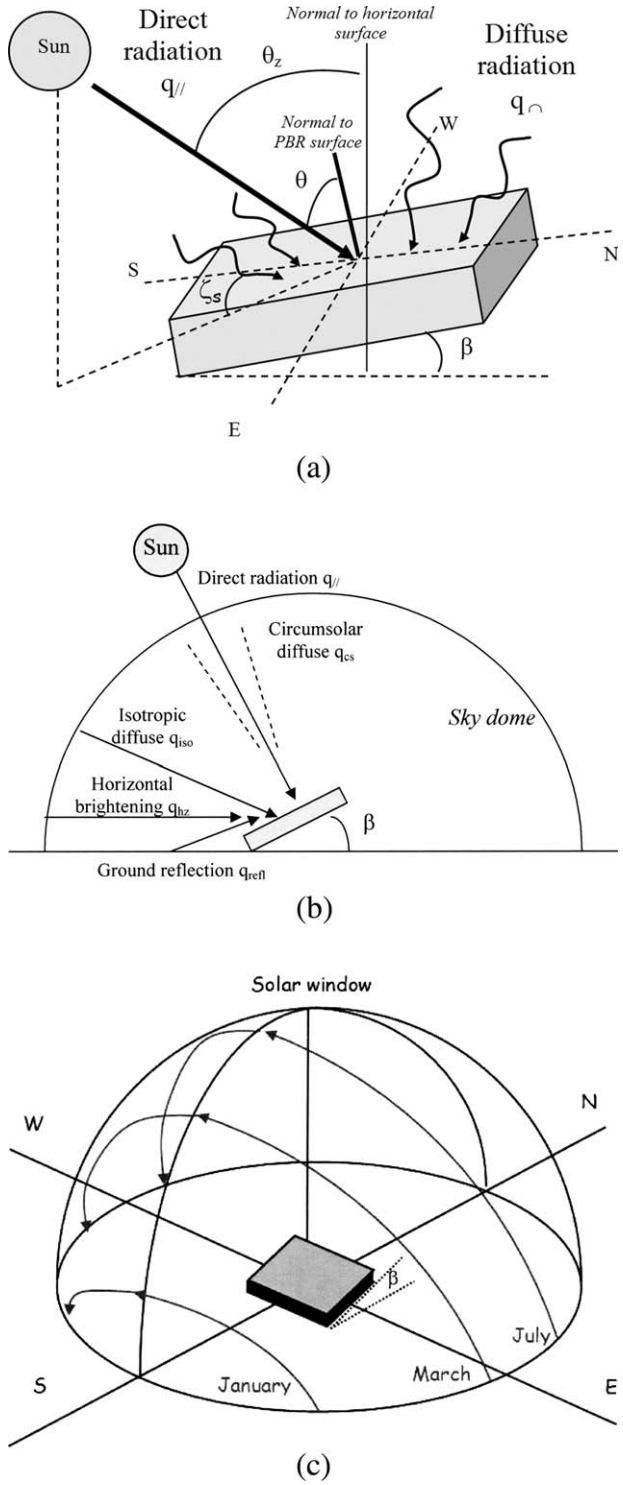

Figure 1. Solar radiation on PBR surface: definition of coordinates (a), diffuse beam radiations received on PBR surface (b), evolution of solar sky path during the year (c).

METEONORM 6.0 software (www.meteonorm.com) was used in this study to generate solar data. For PBR simulation, these data were the total solar radiation q (corresponding to the PFD), the direct radiation $q_{//}$, the total diffuse radiation $q_{\cap}$, and the incident angle θ. This can be calculated for any given surface inclination β and orientation as defined by the solar azimuth angle ζ_s (usually expressed with respect to the south direction). As shown later, it is also of interest to consider the direct normal radiation ($q_{\perp}$), as defined by the beam radiation received on the surface but with normal incidence. This corresponds to the maximum beam radiation that can be collected for a given radiation condition. In the case of a surface positioned in the south direction (Figure 1a), direct radiation ($q_{//}$) and normal direct radiation ($q_{\perp}$) are linked by

$$q_{//} = q_{\perp}[\sin(\beta)\sin(\theta_z)\cos(\zeta_s) + \cos(\beta)\cos(\theta_z)] = q_{\perp}\cos(\theta) \quad (1)$$

with θ_z the zenith angle corresponding to the angle of incidence of direct radiation on a horizontal surface (for horizontal PBR, $\theta_z = \theta$).

The available data involve the whole solar spectrum at the ground level (0.26–3 μm), whereas only the visible part of this radiation is useful for photosynthesis. In what follows, we thus deal with only the photosynthetically active radiation (PAR) of incident light flux densities (0.4–0.7 μm) corresponding to almost 43% of the full solar energy spectrum.

Studies were conducted for averaged summer and winter days. These days corresponded to a month averaging of the 31 days of July for summer and January for winter. The plane PBR was oriented north-south and located in the west of France (St-Nazaire, 47°12N, 01°33W). Corresponding data for incident PFD (in the PAR) are given in Figure 2 for their time courses and in Table 1 for corresponding daily averaged values. For horizontal PBR ($\beta = 0$), very different radiation conditions were obtained, with almost twice less radiation in winter. A different distribution between diffuse and direct components was also obtained. About 50% of the total radiation was diffuse in summer (typical of a clear day, Figure 2a). In winter, it accounted for most of the light intercepted (Figure 2b). These values were also fully dependent on the incident angle. For the horizontal position investigated, normal incidence ($\theta = 0°$) was never achieved, with at best an incident angle tending toward 30° in summer (Figure 2a). The winter period was characterized by $\theta > 70°$ (Figure 2b). This explains the very low direct radiation intercepted. This was confirmed by the normal beam radiation $q_{\perp}$, which was found to be twice higher on average than direct radiation $q_{//}$.

It is interesting to compare these values with the maximum available solar radiation q_{max}; this value, independent of the PBR orientation, is given by the sum of total diffuse $q_{\cap}$ and normal beam radiation $q_{\perp}$. For the summer day, the total radiation q intercepted for a horizontal position was 78% of the total available radiation q_{max}. For the winter day, this value fell to 53%. This difference was fully explained here by the solar sky path, with a lower solar angle of elevation (as represented schematically in Figure 1c), which did not favor a horizontal inclination. As shown in Figure 2c, tilting the PBR with an inclination $\beta = 45°$ resulted in a better incident angle and a significant increase in light capture. The total radiation intercepted was then 88% of the total available radiation.

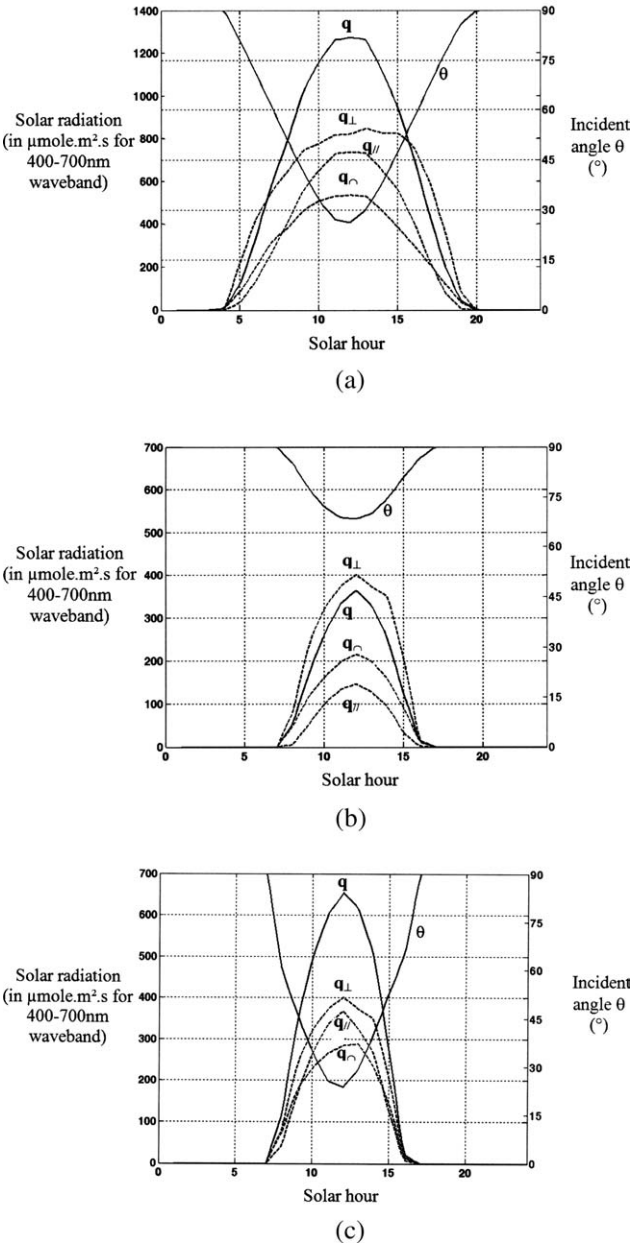

Figure 2. Day–night variations of incident angle and radiation received on PBR surface: horizontal inclination and averaged summer (a) and winter days (b); tilted PBR ($\beta = 45°$) for averaged winter day (c).

Data location is Saint-Nazaire (France).

Radiative transfer modeling inside the culture

Owing to absorption and scattering by cells, light distribution in PBRs is highly heterogeneous. The two-flux model[36,41,42] was applied in this study as a first good approximation of the field of irradiance inside the culture (see Appendix for a full discussion). Its application to the solar case implies taking into account non-normal incidence and treating the direct and diffuse components of the radiation separately. In Cartesian coordinates, the irradiance field for collimated radiation is represented by the following analytical solution (see Ref. 36 and discussion in Appendix)

$$\frac{G_{\mathrm{col}}}{q_{//}} = \frac{2}{\cos\theta}\frac{(1+\alpha)\exp[-\delta_{\mathrm{col}}(z-L)] - (1-\alpha)\exp[\delta_{\mathrm{col}}(z-L)]}{(1+\alpha)^2\exp[\delta_{\mathrm{col}}L] - (1-\alpha)^2\exp[-\delta_{\mathrm{col}}L]}, \tag{2}$$

with the two-flux collimated extinction coefficient $\delta_{\mathrm{col}} = \frac{\alpha C_X}{\cos\theta}(E_a + 2bE_s)$ and $\alpha = \sqrt{\frac{E_a}{(E_a+2bE_s)}}$ the linear scattering modulus. E_a and E_s are, respectively, the mean (spectrally averaged onto the PAR) mass absorption and scattering coefficients for the cultivated photosynthetic microorganism, b the backward scattering fraction, and C_x the biomass concentration in the culture medium.

For a diffuse radiation, the following equation is obtained

$$\frac{G_{\mathrm{dif}}}{q_{\cap}} = 4\frac{(1+\alpha)\exp[-\delta_{\mathrm{dif}}(z-L)] - (1-\alpha)\exp[\delta_{\mathrm{dif}}(z-L)]}{(1+\alpha)^2\exp[\delta_{\mathrm{dif}}L] - (1-\alpha)^2\exp[-\delta_{\mathrm{dif}}L]}, \tag{3}$$

with $\delta_{\mathrm{dif}} = 2\alpha\, C_X\,(E_a + 2b\,E_s)$ the two-flux diffuse extinction coefficient.

The total irradiance is finally given by simply summing the collimated and diffuse components

$$G(z) = G_{\mathrm{col}}(z) + G_{\mathrm{dif}}(z). \tag{4}$$

Equations 2 and 3 show that penetrations of collimated and diffuse radiations inside the bulk culture are widely different. We note that the incident angle θ influences only the collimated part, diffuse radiation being assumed to have an isotropic angular distribution on the illuminated surface (more details on radiative transfer calculation are given in the Appendix, with the influence on productivities of the different assumptions that could be applied in the radiative model).

For this study, the values of $E_a = 162\ \mathrm{m^2\ kg^{-1}}$, $E_s = 636\ \mathrm{m^2\ kg^{-1}}$, and $b = 0.03$ were retained as radiative properties of *Arthrospira platensis*.[20] To simplify the model description, it was decided here to work with spectrally averaged values (absorption and scattering coefficients, backscattered fraction, irradiances, and incident hemispherical PFD) on the

Table 1. Values of Solar Day Averaged PFD Received on PBR Surface for the Different Cases Investigated

Averaged Intercepted Radiation (for PAR) (μmol m^{-2} s^{-1})	Total Radiation q ($q_{//} + q_{\cap}$)	Direct Radiation $q_{//}$	Diffuse Radiation $q_{\cap}$	Direct Normal Radiation $q_{\perp}$	Total Available Radiation $q_{\max}$ ($q_{\perp} + q_{\cap}$)
Summer day, $\beta = 0°$	470	258	212	388	600
Winter day, $\beta = 0°$	82	30	52	102	154
Winter day, $\beta = 45°$	156	82	73	102	175

PAR. All irradiation data derived from Meteonorm were corrected accordingly, these values being expressed by default on a whole solar spectrum basis. For a more accurate representation, but with an increased computational effort, the irradiance field can be solved spectrally, taking into account the spectral distributions of solar radiation and of optical properties of photosynthetic microorganisms (as already applied for artificial light[36]).

The irradiance distribution allows us to determine a significant parameter in PBR engineering, the illuminated fraction γ.[19,20,43] Schematically, the bulk culture can be delimited into two zones, an illuminated zone and a dark zone. Partitioning is obtained by a compensation irradiance value G_c corresponding to the minimum value of radiant energy required to obtain a positive photosynthetic growth rate (the "compensation point" for photosynthesis defined from oxygen exchange rate measurements at a local and fast typical dynamic of electron carriers chains functioning). In the one-dimensional rectangular case, the working illuminated fraction γ is then given by the depth of the culture z_c where the irradiance of compensation $G(z_c) = G_c$ is obtained by

$$\gamma = \frac{z_c}{L}. \tag{5}$$

For *A. platensis*, this value was calculated and experimentally measured to give $G_c = 1.5\ \mu\text{mol m}^{-2}\ \text{s}^{-1}$.[44] Two examples of light fraction γ determination are given in the Appendix.

Values of γ below 1 indicate that all the available light for photosynthesis received is absorbed by the culture. Conversely, when the illuminated fraction is greater than 1, some of the light is transmitted (kinetic regime). It was recently confirmed by the authors that PBR performance of any light-limited PBR was strictly linked to this γ fraction.[19,20] Because it does not allow full absorption of the light captured, the kinetic regime always leads to a loss of efficiency ($\gamma > 1$). Full light absorption is thus to be preferred ($\gamma \leq 1$). In the case of cyanobacteria cultivation, this allows maximal productivity.[20] Although not considered here, it must be noted that for eukaryotic (microalgae) microorganisms presenting respiration in the light, a dark zone in a PBR will result in a loss of productivity due to respiration.[19] Maximal productivity will then require the γ fraction to fulfill the exact condition $\gamma = 1$ (the "luminostat" regime), corresponding to a full absorption of the light received but without a dark zone in the PBR.[22,45]

Kinetic modeling of photosynthetic growth

As a common species with several industrial applications (food, proteins, and pigments), with a production in solar conditions widely described in literature,[21,46] growth of the cyanobacteria *A. platensis* was considered for simulations (but the method could be extended to any other cultivated species with an appropriate kinetic growth model and radiative properties). A kinetic model validated on a large number of artificial light PBRs was recently proposed for this species.[44,47] It enables the predictive calculation of the mean volumetric growth rate in light-limited conditions $\langle r_x \rangle$, as a result of the respective contribution of the illuminated and dark zones for any given PBR. Those zones can be defined with respect to the illuminated fraction γ and the location of the compensation point, as deduced from radiative transfer modeling

$$\langle r_X \rangle = \gamma \frac{1}{z_C} \int_0^{z_c} r_{x,l}.\mathrm{d}z + (1-\gamma) \frac{1}{(L - z_c)} \int_{z_C}^{L} r_{x,d}.\mathrm{d}z, \tag{6}$$

where $r_{X,l}$ represents the local volumetric growth rate in the illuminated zone (from optical surface to the location of the compensation point). This photosynthetic growth is linked to the local radiant light power density absorbed A and thus the local value of irradiance G inside the PBR, following

$$r_{X,l} = \rho \bar{\phi} \mathcal{A} = \rho_M \frac{K}{K+G} \bar{\phi} E_a G C_X, \tag{7}$$

in which $\rho_M = 0.8$ is the maximum energy yield for photon dissipation in the antenna, $\bar{\phi} = 1.85 \times 10^{-9} \text{kg}_x \cdot \mu\text{mol}_{h\upsilon}^{-1}$ is the mean spatial quantum yield for the Z-scheme of photosynthesis, and $K = 90\ \mu\text{mol}_{h\upsilon}\ \text{m}^{-2}\ \text{s}^{-1}$ is the half saturation constant for *A. platensis*.[20]

In Eq. 6, $r_{x,d}$ represents the volumetric growth rate in the dark. For cyanobacteria like *A. platensis* that have common electron carrier chains for photosynthesis and respiration, it is necessary to consider the relaxation time necessary to switch the metabolism from photosynthesis to respiration, which is of the order of magnitude of several minutes.[48] Although a large dark zone can occur in light-limited growth, mixing along the light gradient causes cells to experience a fluctuating light regime when flowing from light to dark zones. For usual conditions of mixing applied in PBRs, residence times in each zone are in the range of a few seconds.[42] In consequence, so long as the PBR is illuminated, $r_{x,d} = 0$ in the PBR dark volume (no respiration corresponding to the consumption of endogenous reserves, and so to biomass growth rate losses, as also assumed for artificial permanent illumination). This value was applied during the day. During the night with long dark periods of several hours, the switch to respiration metabolism occurs. The resulting biomass catabolism can be represented by introducing a negative biomass volumetric rate of production. For *A. platensis*, a value of $\langle r_x \rangle / C_X = \mu = 0.001\ \text{h}^{-1}$ was measured at 36°C.[49] This constant specific rate was applied during the night. Partition between day and night was defined using the irradiance of compensation G_c. When irradiation received on the PBR surface was found to be below G_c, night period was considered.

Solving of PBR behavior in solar conditions and areal productivity

The biomass concentration C_x can be obtained by a standard mass balance on a continuous PBR assuming perfectly mixed conditions

$$\frac{\mathrm{d}C_X}{\mathrm{d}t} = \langle r_X \rangle - \frac{C_X}{\tau}, \tag{8}$$

with τ the residence time for the PBR resulting from the liquid flow rate of the feed (fresh medium) and $\tau = 1/D$ (D being the dilution rate).

The mean volumetric growth rate $\langle r_x \rangle$ was determined as described in the previous section. Because of the time course of solar conditions, Eq. 8 has to be solved in its transient form (using the routine *ode23tb* in the Matlab software).

Values of biomass concentration C_X were then used to determine PBR productivity. We elected to express productivity per unit of illuminated surface (dividing $\langle r_X \rangle$ by the specific illuminated area $a = 1/L$). Areal productivity is a useful variable for extrapolation to land area production. In addition, it has also been shown that maximal performance of a PBR (in light-limited conditions) when expressed on a surface basis was independent of the cultivation system design.[22] This is not the case for the volumetric biomass productivity, which is closely linked to PBR geometry and its specific illuminated surface. The instantaneous surface biomass productivity $\langle s_x \rangle$ is then defined by

$$\langle S_X(t) \rangle = \frac{C_X(t) D V_r}{S_L} = \frac{C_X(t) L}{\tau}, \tag{9}$$

with V_r the PBR culture volume and S_L the illuminated surface.

Calculation of optimal areal productivity for solar surface-lightened PBR

Achievement of maximal productivities in PBR has been discussed and demonstrated theoretically[20] and experimentally[19] by the authors but for artificial permanent illumination. This approach was demonstrated to work with only physical limitation by light. With a correct choice of the illuminated fraction γ (as discussed previously), the maximal PBR productivity can be reached for a given species, and is then found to depend only on the incident PFD.[22] In solar conditions, as incident flux densities vary with time (boundary conditions), maintaining optimal light attenuation conditions at each moment of the day would be very difficult. In addition, fixed PBRs will not be able to collect all available solar energy due to the earth's rotation. Thus, it is desirable to distinguish between maximal productivity achieved for a given PBR with a defined light interception as fixed by its geometry, orientation, and inclination, and the optimal productivity that could be reached assuming optimal capture and biological use of available solar energy throughout the day. The ratio of the two productivities will then define the PBR efficiency for given solar conditions. If applied to the areal productivity (a value found to be independent of the PBR geometry as explained above), optimal areal productivity will also define the upper limit for the species cultivated under given solar irradiation conditions (restricted here to surface-lightened PBRs, volumetrically lightened PBRs giving rise to a higher limit of productivity; see Ref. 22 for details). Optimal areal productivity is obtained with the following three assumptions:

(i) optimal capture: all available solar radiation is hypothetically collected at each moment of the day. This means that both diffuse $q_\cap$ and direct $q_\perp$ parts of solar radiation are collected with normal incidence ($\theta = 0$) at each moment.

(ii) optimal PBR running (see Ref. 22): optimal light absorption conditions inside the culture are maintained throughout the day. For prokaryotic cells, this implies only full light absorption ($\gamma \leq 1$). For eukaryotic cells, due to respiration in light, the condition of no dark zone in the bulk culture has to be added ($\gamma = 1$). Obviously, no limitation other than light occurs (no mineral or carbon limitation, optimal temperature, and pH conditions).

(iii) ideal biological response: there are no adverse effects of strong light on photosynthetic conversion (no photoinhibition). In addition, there is no biomass loss during night due to respiration.

These three conditions can be easily introduced into the model. Condition (i) implies only the correct definition of the PFD received, thus giving the total available solar radiation $q_{max} = q_\cap + q_\perp$. Condition (ii) requires a specific calculation for each variation of the light received. The optimal biomass concentration is determined so as to obtain ideal attenuation condition as represented by an illuminated fraction $\gamma = 1$ and $\gamma \leq 1$ for eukaryotic and prokaryotic cells, respectively. As a common constraint to both organisms, the $\gamma = 1$ condition (luminostat regime) was retained here (same results for cyanobacteria with $\gamma \leq 1$). Equation 4 is solved so as to obtain the biomass concentration C_X leading to $G(L) = G_c$. Condition (iii) is simply obtained by maintaining $r_{x,d} = 0$ during the night and by applying Eqs. 6 and 7 for daytime.

Results and Discussion

Determination of maximal areal productivity and investigation of continuous and semi-continuous harvesting in summer

For a given species and geometry, PBR productivity depends on the harvesting strategies (defined by the harvesting period and by the dilution rate D or residence time $\tau = 1/D$, applied). In the conditions of light limitation, this is a function of the incident PFD, and this problem may be examined by solving Eqs. 8 and 9 for given values of the residence time τ.

Two examples of simulation results are presented in Figure 3 for a horizontal PBR and for an averaged summer day. Simulations were conducted for the PBR with continuous harvesting and for two residence times, $\tau = \tau_{opt} = 2.7$ days, giving the maximal areal productivity (its determination is described below) and for an arbitrary value of the residence time $\tau = \tau_{opt}/2$. Results show the direct influence of the residence time on resulting biomass concentration evolution and corresponding areal productivities, as a classical, direct consequence of culture dilution when residence time in the reactor is varied.

In permanent illumination conditions (artificial light), the PBR is usually operated in continuous mode, with a constant, permanent value of the residence time τ. For practical reasons, many solar mass scale PBRs are operated even in batch mode with biomass harvesting at the end of the culture, or in semi-continuous mode with spot harvesting of part of the culture and its replacement by fresh growth medium. All methods can be simulated using the model presented in this study by choosing an appropriate formulation of the residence time in Eq. 8. Continuous and semi-continuous productions were compared here by, respectively, applying a constant residence time for continuous harvesting over the 24-h period, and a time-varying value of the residence

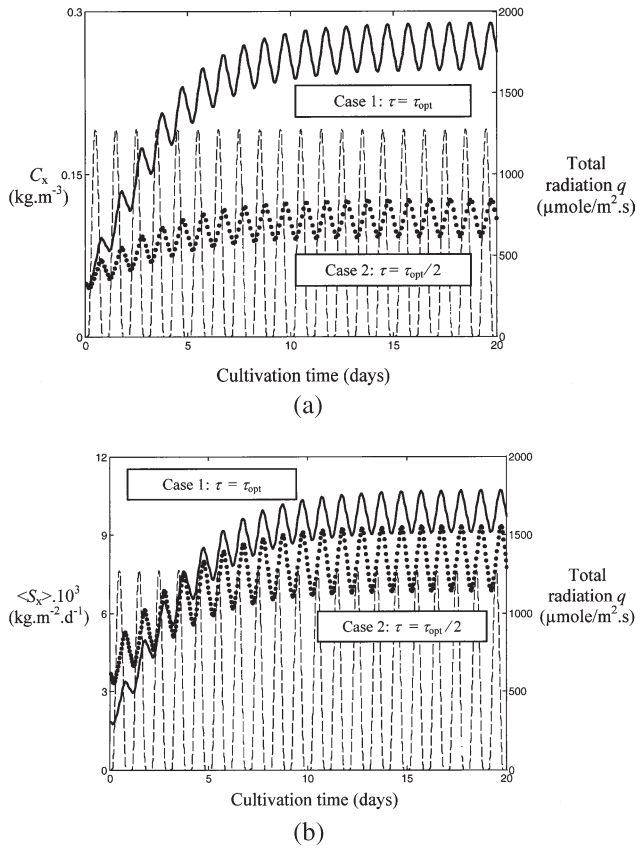

Figure 3. Time resolution of biomass concentration (a) and areal productivity (b) evolution for a horizontal rectangular PBR and averaged summer day (location Saint-Nazaire).

The PBR was operated with continuous harvesting and results are given for two residence times $\tau = \tau_{opt}$ (solid line) and $\tau = \tau_{opt}/2$ (dotted line), with $\tau_{opt} = 2.7$ days, the optimal residence time giving the maximal areal productivity (see text for details). Total radiation received on the PBR surface is also given (dashed line).

time for semi-continuous mode. For the latter case, this was retained to alternate between batch ($\tau = \infty$ or $D = 0$) and harvesting periods at a given residence time, with harvesting during the day period 11:00–13:00 h. To facilitate comparison with permanent harvesting, the residence time was averaged over the entire day, thus giving the fraction of reactor volume harvested per day, independently of the harvesting protocol used. If needed, the instantaneous residence time applied during the harvesting period for semi-continuous mode could be obtained easily by correcting the daily averaged value with respect to the fraction of the 24-h period devoted to harvesting (1/6 in this case).

The two harvesting methods were compared here for the averaged summer day. The results are given in Figure 4 for both continuous and semi-continuous modes. The optimal residence time corresponding to the maximal productivity is easily observed ($\tau_{opt} = 2.7$ days, thus corresponding to a dilution rate $D = 1/\tau = 0.37$ day^{-1}). More interestingly, we observed that almost the same maximal productivities (the small discrepancy will be explained in the next section) and optimal residence times were obtained, irrespective of the harvesting procedure (if residence times are expressed on a full-day basis, as described above). A parallel can be made with results obtained with permanent artificial illumination, where maximal productivity for light-limited growth was found to depend only on the incident light flux[19,20] for a given design of the PBR (i.e., the specific illuminated area a). The same was observed here in natural varying light conditions, with maximal productivity set by the irradiation conditions. Finally, we see in Figure 4 a slight optimum in productivity, with a slight decrease for values of τ higher than τ_{opt}. As shown in the next section, this results from the optimization procedure, which considers a first-order biomass concentration decrease during the night. Increasing τ and thus the biomass concentration results in a higher biomass loss during the night, resulting from an optimal value of the residence time τ (or biomass concentration). This emphasizes the utility of developing accurate kinetic models for respiration at night, mainly for eukaryotic microorganisms for which this issue, coupled to respiration in light, is of crucial importance.

PBR transient response to solar conditions

Figure 5 presents the daily variation of biomass concentration and of the γ fraction as obtained when the optimal residence time was applied. Results are given for both continuous and semi-continuous harvesting procedures and for the horizontal PBR in summer, as defined in the previous section. Results of simulations emphasize the direct relation between light supply and cultivation (and thus PBR) response. Biomass decreases during the night owing to cell respiration (catabolism) and starts to increase again at sunrise. The biomass then increases continuously throughout the day, decreasing only at nightfall (22:00 h in summer). There is thus a time lag between the maximum of incident light flux (12:00 h) and the biomass concentration. This confirms that light limitation occurs, with a decrease in biomass concentration only very late in the day (around 21:00 h), when

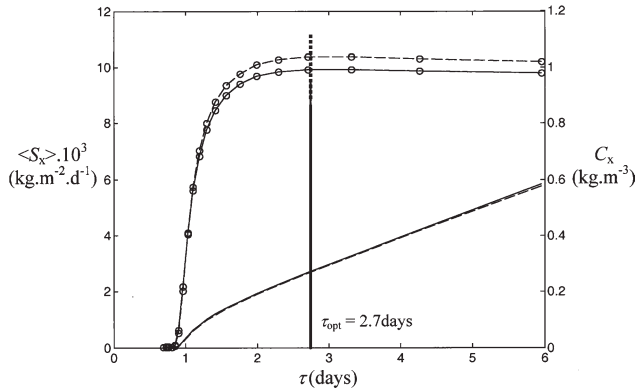

Figure 4. PBR areal productivity (circles added on lines) and corresponding biomass concentration (no circle) as a function of residence time, for continuous (solid line) and semi-continuous (dashed line) harvesting (averaged summer day, location Saint-Nazaire).

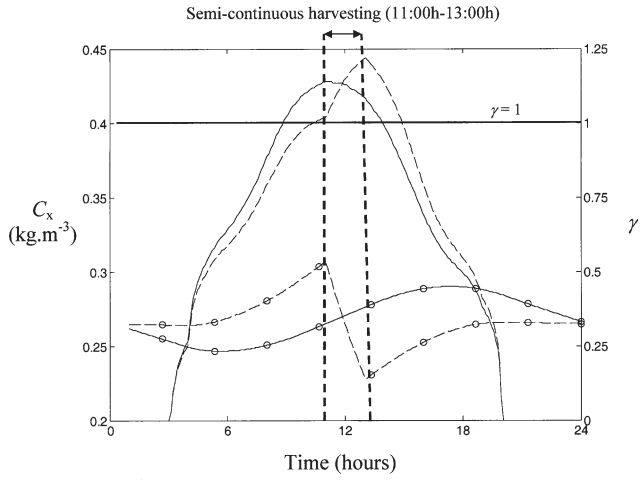

Figure 5. Day–night variations of biomass concentration (circles added on lines) and illuminated fraction (no circle) for continuous (solid line) and semi-continuous (dashed line) harvesting (averaged summer day, location Saint-Nazaire).

the incident light flux becomes too low to maintain positive growth.

If continuous and semi-continuous harvesting procedures are compared, different time courses of biomass concentration are observed, with a discontinuous variation between 11:00 and 13:00 h for the semi-continuous procedure, as a direct effect of biomass harvesting. As a result, different light absorption conditions inside the PBR were obtained, as shown by the γ fraction. For both harvesting procedures, all the light was absorbed during the main part of the day ($\gamma < 1$) except at noon when transmission through the culture occurred ($\gamma > 1$). As previously explained, this situation arises from the optimization procedure of biomass productivity along a cycle. The biomass decrease at night is proportional to the maximum biomass concentration reached at the end of the day (first order), resulting in a lower daily optimal concentration, responsible also for the kinetic regime appearance ($\geq$1), biomass dilution by harvesting favoring light transmission. Because the harvesting procedure directly affects biomass concentration, it can be used to optimize light absorption by the culture. This is shown in Figure 4, semi-continuous harvesting giving rise to a slightly higher PBR productivity, owing to a higher biomass-concentration at the end of the morning, which guarantees full light absorption before harvesting. This didactic example illustrates one difficulty of working with dynamic solar illumination and variable photoperiods (different durations of day–night cycles), which require advanced control strategies. The simulation of PBR dynamic behavior proposed in this work is therefore helpful. It can be used to define harvesting conditions and so optimize light attenuation conditions (as represented by γ) or, of more practical concern, downstream processing if influenced by the biomass concentration in the harvest.

Investigation of the winter period

As a second example, an averaged day of winter was simulated (results are given only for the simplest case of continuous harvesting over a 24-h period). Figure 6a shows that the optimal residence time was in this case $\tau_{opt} = 5.3$ days, giving a maximal daily averaged areal productivity of 2.8 g m^{-2} d^{-1} lower than in summer (10 g m^{-2} d^{-1}). This confirms the primary relevance of illumination conditions not only on PBR productivity (a classical result) but also on its optimal operation, with a value of τ_{opt} that is greatly modified ($\tau_{opt} = 2.7$ days in summer), emphasizing the need to adapt this value during the year to maintain maximal system performance. The day–night variation of biomass concentration is shown in Figure 6b when working at optimal residence time in winter. The illuminated light fraction time course illustrates the wide variation of light conditions during the day and emphasizes that the optimization of the productivity in winter leads to a longer period under the kinetic regime ($\gamma > 1$). This stems indirectly from the more marked biomass concentration decrease at night with 16 h per day in the dark (in the corresponding example), leading to choose a lower optimal biomass concentration at the end of the

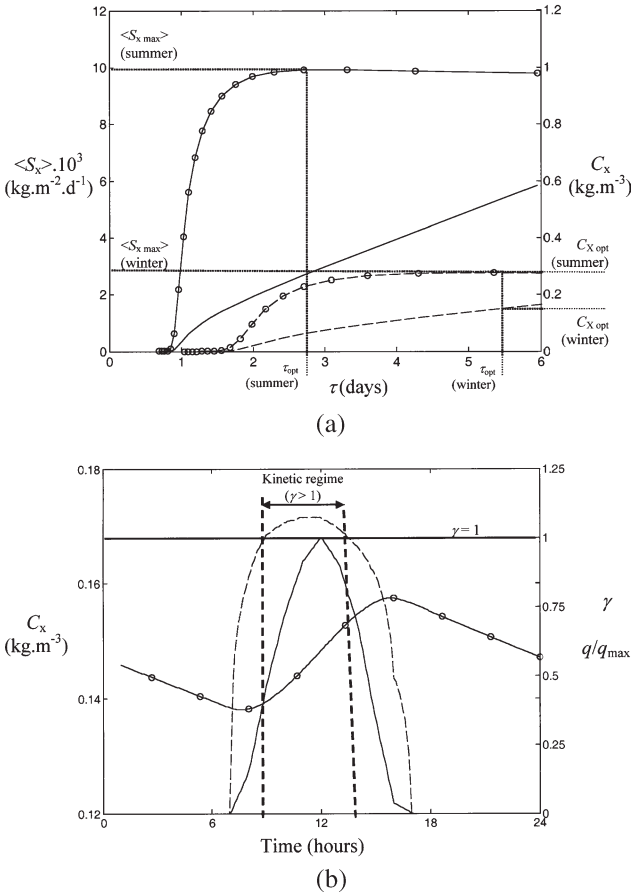

Figure 6. Results of simulations for a horizontal PBR for averaged winter day.

(a) Gives the areal productivity and corresponding biomass concentration as a function of residence time, for averaged summer (solid line) and winter day (dashed line). (b) Gives the day–night variations for optimal residence time of biomass concentration (solid line and circles), the illuminated fraction (dashed line), and the normalized PFD (solid line).

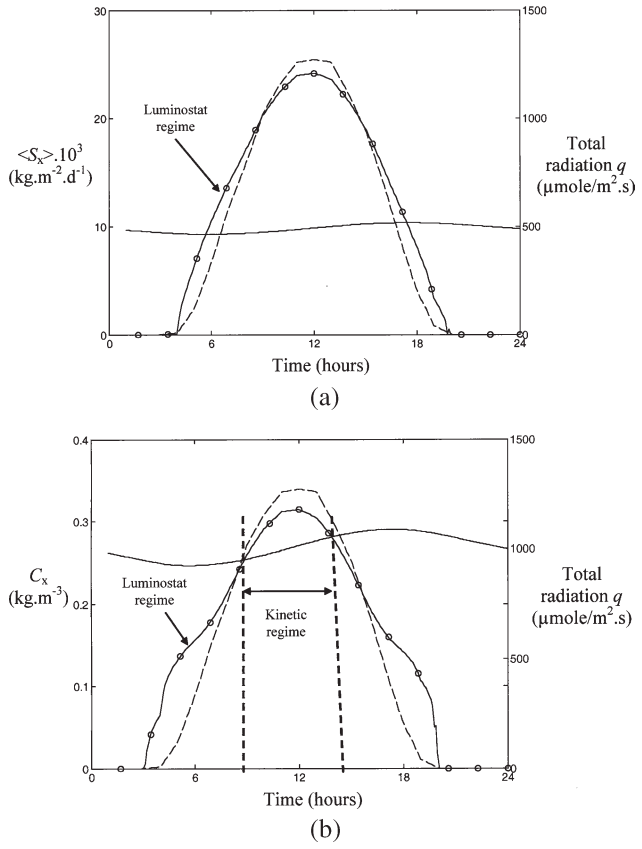

Figure 7. Comparison of the dynamic operation of the PBR as a response to day–night cycles with (solid line and circles) and without assuming a luminostat regime (solid line).

Results are given for day–night variations of areal productivity (a). and biomass concentration (b). The total radiation is also represented (dashed line). Simulations were conducted for horizontal inclination and averaged summer day.

illuminated period. As a consequence, the optimal productivity was reached with a higher duration of the kinetic regime than in summer (about 25% of the day period in summer against 70% in winter). This contributed, with the reduction of available solar energy in winter, an additional decrease in PBR productivity, ultimately resulting in a more strongly reduced efficiency during that period (a more detailed analysis of productivity is given below).

Because it leads to a decrease in light conversion by the process, the kinetic regime is ideally avoided in PBR. This implies obtaining a sufficiently high biomass concentration to absorb all the intercepted PFD. In solar conditions with permanent variation and a certain degree of unpredictability (clouds, etc.), this will be very difficult. As shown previously in Figure 3, the modification of the residence time led to different biomass concentration time courses, with only a small influence on resulting areal productivity. As it is easy to modify in practice (it is set only by the feed flow rate), the residence time thus proves to be a parameter of interest to optimize during day–night cycles. In this study, the case is obviously oversimplified (simulation of an infinite succession of the same day and permanent harvesting). However, based on the same theoretical framework, advanced control strategies could be developed to keep the PBR running close to its optimal productivity, taking into account time variation of illumination conditions as a result of not only day–night cycles but also meteorological conditions. The utility of this approach has already been demonstrated in the context of artificially lightened PBRs.[50]

Comparison with the luminostat regime

To emphasize the specific transient PBR regime as imposed by day–night cycles, results of simulations were compared with a hypothetical luminostat regime (results given only for the summer day, same conclusion for the winter day). By definition, this corresponds to the maximal PBR productivity, as would be obtained when operating the PBR at steady state and at optimal residence time in a permanent illumination condition (this case is purely theoretical here, the practical application of a luminostat regime in real solar conditions being beyond the scope of this study). When applied to the day–night cycles (Figure 7a), the luminostat regime gave a time course that perfectly followed the daily variation of incident light flux, with an increase in biomass production until noon, and then a decrease to nil during the night. This was thus markedly different from the transient PBR behavior described in the previous section. Compared with productivities of the luminostat regime, instantaneous productivities were found to have small amplitude. Because the luminostat regime when applied to a day–night cycles can be regarded as a succession of optimal steady states of the PBR, this again confirms the very low dynamics of the process. As shown in Figure 7b, biomass concentration oscillated near a quasi-constant value, very different from the one that would be obtained assuming a steady state regime for each value of the PFD received during the day. The specific transient response with small amplitude is here fully explained by the low kinetics of algae growth compared with day–night cycles.

It is interesting to correlate those time courses with the corresponding daily averaged areal productivities. Despite a marked difference in the dynamics of instantaneous values, almost the same daily averaged areal productivity was obtained in the luminostat regime as the maximal value determined in the previous section, with only a 5% gain with the luminostat regime (10.5 g m^{-2} d^{-1} against 10 g m^{-2} d^{-1}). Although instantaneous response was far from optimal, the PBR ran near a pseudo steady state with a mean productivity close to optimal. This confirms the previous conclusions of the authors[19] obtained with artificially illuminated PBRs enabling an accurate control of radiation field. They postulated that a deviation of the illuminated fraction γ by 15% was responsible for only slight variations in the biomass productivity. This conclusion certainly also illustrates a general optimization of photosynthetic growth in day–night natural cycles. However, this has to be related to the species considered: *A. platensis*, as a prokaryotic photosynthetic microorganism, is weakly influenced by dark zones (no respiration in light) and night (low respiration rate). This would certainly be very different for eukaryotic cells such as microalgae, which respire even when illuminated, resulting in a

Table 2. Summary of Day Averaged Maximal and Optimal Areal Productivities, PBR Efficiency, and Light Interception for the Different Cases Investigated (See Text for Details)

Areal Productivity (10^3 kg m^{-2} d^{-1})	Maximal Productivity	Optimal Productivity	PBR Efficiency (%)	Light Interception Yield (%)
Summer day, $\beta = 0°$	10	15	66	78
Winter day, $\beta = 0°$	2.8	6.3	44	53
Winter day, $\beta = 45°$	4.7	6.3	74	89

significant negative influence of dark zones on PBR productivity (biomass catabolism). As already observed in artificially lightened PBRs, a more marked difference would certainly be observed for such microorganisms when not working in optimal light absorption conditions ($\gamma = 1$). As shown in Figures 7b and 6b, such a condition is only fulfilled during very brief periods.

Areal productivities and utility of maximizing radiation interception

Maximal productivities were determined for the various conditions investigated (summer and winter day, for a horizontal and tilted surface with an inclination $\beta = 45°$ in winter). Productivities assuming optimal light interception and biological use of available solar energy were also calculated. By definition, this gives the optimal productivity achievable for the irradiation conditions investigated, independently of the PBR geometry and orientation. All results are summarized in Table 2. Productivity of the horizontal PBR in summer was 66% of the optimal value. This is mainly explained by sunlight capture, which accounts for 78% of the available solar irradiation. The effect of night on biomass loss, or not working at optimal absorption conditions in the luminostat regime, was shown here to have only a small influence. However, as stated above, this conclusion must be related to the microorganism investigated (*A. platensis*), which proves to be poorly influenced by night or dark zones in the PBR.

Productivities in winter showed a marked reduction in productivity compared with summer. This was expected but also illustrates the fact that extrapolation of summer productivity to a whole year (as sometimes found in the literature) is risky. It is again interesting to correlate results of productivities to the irradiation intercepted by the PBR. The horizontal position allowed interception of only 53% of the available light energy in winter owing to the low elevation of the sun path during winter (high incident angle on PBR surface). As a result, areal productivity was only 44% of the optimal value. Interception could be increased by simply tilting the PBR. Tilting the surface with an inclination $\beta = 45°$ (roughly the latitude of the city of St-Nazaire) greatly modified the incident angle of solar radiation on the PBR surface and increased irradiation interception by 90% compared with the horizontal configuration (see Figure 2c and Table 1). Maximal areal productivity achieved in these conditions was 4.7 g m^{-2} d^{-1}, representing 74% of the optimal value. This result clearly illustrates the utility of maximizing irradiation interception.

Conclusions

As for any solar processes, PBR operation and productivities are closely dependent on irradiation conditions. A generic model is proposed that represents light-limited growth in solar PBRs. Using a theoretical framework derived from many years of investigation in artificial light PBRs, this model was extended to take into account specific features of dynamic solar radiation, such as variation of incident angle or direct/diffuse distribution of sunlight flux density. The model was associated with a solar database to predict solar PBR areal productivity as a function of PBR ability to intercept solar radiation, and PBR transient behavior as a combined result of solar cycles and growth kinetics, both having different dynamics that prevent a steady state being obtained.

As already shown, especially for artificial light systems, modeling is a necessary framework to integrate the interdependent, complex features governing PBRs (radiative transfer conditions inside the culture and photosynthetic conversion by the cultivated species) in which photonic conversion occurs inside the bulk culture. This was especially evident for the solar case, solar radiation interception and the resulting transient behavior of the process making analysis more complex. The extension of a modeling approach to the solar case will thus help to improve our knowledge of this particular type of PBR. Future studies will use this model as a basis for the specific investigation of solar PBRs, such as PBR behavior under more realistic day–night cycles as encountered over a full year, the optimization of PBR geometry (and especially with regard to light interception), or the development of advanced control strategies to optimize light use during day–night cycles. The model will also be extended to heat transfer, to predict temperature evolution during day–night cycles (another major practical limitation of solar PBRs).

Acknowledgments

This work was supported by the French National Research Agency for Bioenergy Production (ANR-PNRB), and is part of the French "BIOSOLIS" research program on developing photobioreactor technologies for mass scale solar production (http://www.biosolis.org/).

Notation

A = local volumetric radiant power density absorbed, μmol s^{-1} m^{-3}
b = back-scattered fraction for radiation, dimensionless
C_X = biomass concentration, kg m^{-3}
D = dilution rate, h^{-1} or s^{-1}
E_a = mass absorption coefficient, m^2 kg^{-1}
E_s = mass scattering coefficient, m^2 kg^{-1}
G = local spherical irradiance, μmol s^{-1} m^{-2}
G_c = compensation irradiance value, μmol s^{-1} m^{-2}
K = half saturation constant for photosynthesis, μmol s^{-1} m^{-2}
L = depth of the rectangular photobioreactor, m
q = total radiation received on photobioreactor surface (same as photon flux density), μmol s^{-1} m^{-2}

r_X = biomass volumetric growth rate (productivity), kg m^{-3} s^{-1} or kg m^{-3} h^{-1}
S_L = illuminated surface of the photobioreactor, m^2
S_X = areal biomass productivity, kg m^{-2} d^{-1}
t = time, days or s
V_r = photobioreactor volume, m^3
z = depth of culture, m

Greek letters

α = linear scattering modulus, dimensionless
β = inclination of the photobioreactor surface, rad
γ = fraction for working illuminated volume in the photobioreactor, dimensionless
δ = extinction coefficient for the two-flux method, m^{-1}
θ = incident angle, rad
θ_z = zenith angle, rad
ρ_M = maximum energy yield for photon conversion, dimensionless
τ = hydraulic residence time, h
$\bar{\phi}$ = mean mass quantum yield for the Z-scheme of photosynthesis, kg_X μmol_{hv}^{-1}
ζ_s = solar azimuth angle, with respect to the south, rad

Subscripts

// = related to beam radiation
$\perp$ = related to normal beam radiation
$\cap$ = related to total diffuse radiation
cs = related to circumsolar diffuse radiation
col = related to collimated part of irradiance
dif = related to diffuse part of irradiance
d = related to a dark zone in the photobioreactor
hz = related to horizon brightening (diffuse radiation calculation)
iso = related to isotropic diffuse radiation received from the sky dome (diffuse radiation calculation)
ℓ = related to an illuminated zone in the photobioreactor
max = related to maximum available solar radiation
opt = related to the optimal value for residence time
refl = related to reflected radiation (diffuse radiation calculation)

Other

spatial averaging = $\langle X \rangle = \frac{1}{V_r} \iiint_{V_r} X \, dV$

Abbreviations

PAR = photosynthetically active radiation
PBR = photobioreactor
PFD = photon flux density

Literature Cited

1. Spolaore P, Joannis-Cassan C, Duran E, Isambert A. Commercial applications of microalgae. *J Biosci Bioeng*. 2006;101:87–96.
2. Ghirardi ML, Zhang L, Lee JW, Flynn T, Seibert M, Greenbaum E, Melis A. Microalgae: a green source of renewable H_2. *Trends Biotechnol*. 2000;18:506–511.
3. Melis A. Green alga hydrogen production: progress, challenges and prospects. *Int J Hydrogen Energy*. 2002;27:1217–1228.
4. Benemann JR. *Hydrogen and methane production by microalgae*. In: Richmond A, editor. *Handbook of Microalgal Culture: Biotechnology and Applied Technology*. Oxford, UK: Blackwell Sciences Ltd, 2004.
5. Scragg AH, Illman AM, Carden A, Shales SW. Growth of microalgae with increased calorific values in a tubular bioreactor. *Biomass and Bioenergy*. 2002;23:67–73.
6. Tsukahara K, Sawayama S. Liquid fuel production using microalgae. *J Jpn Pet Inst*. 2005;48:251–259.
7. Carvalho AP, Meireles LA, Malcata FX. Microalgal reactors: a review of enclosed system designs and performances. *Biotechnol Prog*. 2006;22:1490–1506.
8. Lehr F, Posten C. Closed photo-bioreactors as tools for biofuel production. *Curr Opin Biotechnol*. 2009;20:280–285.
9. Richmond A. Principles for attaining maximal microalgal productivity in photobioreactors: an overview. *Hydrobiologia*. 2004;512:33–37.
10. Ugwu CU, Aoyagia H, Uchiyamaa H. Photobioreactors for mass cultivation of algae. *Bioresour Technol*. 2008;99:4021–4028.
11. Daniel KJ, Laurendeau NM, Incropera FP. Prediction of radiation absorption and scattering in turbid water bodies. *J Heat Transfer*. 1979;101:63–67.
12. Houf WG, Incropera FP. An assessment of techniques for predicting radiation transfer in aqueous media. *J Quant Spectrosc Radiat Transfer*. 1980;23:101–115.
13. Incropera FP, Thomas JF. A model for solar radiation conversion to algae in a shallow pond. *Sol Energy*. 1978;20:157–165.
14. Cornet JF, Favier L, Dussap CG. Modeling stability of photoheterotrophic continuous cultures in photobioreactors. *Biotechnol Prog*. 2003;19:1216–1227.
15. Fouchard S, Pruvost J, Degrenne B, Titica M, Legrand J. Kinetic modeling of light limitation and sulphur deprivation effects in the induction of hydrogen production with Chlamydomonas reinhardtii Part I. Model description and parameters determination. *Biotechnol Bioeng*. 2009;102:132–147.
16. Pruvost J, Van Vooren G, Cogne G, Legrand J. Investigation of biomass and lipids production with *Neochloris oleoabundans* in photobioreactor. *Bioresour Technol*. 2009;100:5988–5995.
17. Martin CA, Sgalari G, Santarelli F. Photocatalytic processes using solar radiation. Modeling of photodegradation of contaminants in polluted waters. *Ind Eng Chem Res*. 1999;38:2940–2946.
18. Rossetti GH, Albizzati ED, Alfano OM. Modeling and experimental verification of a flat-plate solar photoreactor. *Ind Eng Chem Res*. 1998;37:3592–3601.
19. Takache H, Christophe G, Cornet JF, Pruvost J. Experimental and theoretical assessment of maximum productivities for the microalgae Chlamydomonas reinhardtii in two different geometries of photobioreactors. *Biotechnol Prog*. 2010;26:431–440.
20. Cornet JF, Dussap CG. A simple and reliable formula for assessment of maximum volumetric productivities in photobioreactors. *Biotechnol Prog*. 2009;25:424–435.
21. Richmond A. *Handbook of Microalgal Culture: Biotechnology and Applied Phycology*. Oxford, UK: Blackwell Sciences Ltd, 2004.
22. Cornet JF. Calculation of optimal design and ideal productivities of volumetrically lightened photobioreactors using the constructal approach. *Chem Eng Sci*. 2010;65:985–998.
23. Zijffers JW, Janssen M, Tramper J, Wijffels RH. Design process of an area-efficient photobioreactor. *Mar Biotechnol*. 2008;10:404–415.
24. Csogör Z, Herrenbauer M, Schmidt K, Posten C. Light distribution in a novel photobioreactor—modelling for optimization. *J Appl Phycol*. 2001;13:325–333.
25. Hsieh CH, Wu WT. A novel photobioreactor with transparent rectangular chambers for cultivation of microalgae. *Biochem Eng J*. 2009;46:300–305.
26. Ogbonna JC, Yada H, Masui H, Tanaka H. A novel internally illuminated stirred tank photobioreactor for large-scale cultivation of photosynthetic cells. *J Ferment Bioeng*. 1996;82:61–67.
27. Acién Fernández FG, Fernández Sevilla JM, Sánchez Pérez JA, Molina Grima E, Chisti Y. Airlift-driven external-loop tubular photobioreactors for outdoor production of microalgae: assessment of design and performance. *Chem Eng Sci*. 2001;56:2721–2732.
28. Oswald WJ. Large-scale algal culture systems (engineering aspects). In: Borowitska MA, editor. Micro-Algal Biotechnology. Cambridge, UK: Cambridge University Press, 1988:357–394.
29. Molina E, Fernández J, Acién FG, Chisti Y. Tubular photobioreactor design for algal cultures. *J Biotechnol*. 2001;92:113–131.
30. Pulz O. Photobioreactors: production systems for phototrophic microorganisms. *Appl Microbiol Biotechnol*. 2001;57:287–293.
31. Chini Zitelli GC, Pastorelli R, Tredici MR. A Modular Flat Panel Photobioreactor (MFPP) for indoor mass cultivation of Nannochloropsis sp. under artificial illumination. *J Appl Phycol*. 2000;12:521–526.
32. Chini Zittelli G, Rodolfi L, Biondi N, Tredici MR. Productivity and photosynthetic efficiency of outdoor cultures of Tetraselmis suecica in annular columns. *Aquaculture*. 2006;261:932–943.
33. Doucha J, Livansky K. Productivity, CO_2/O_2 exchange and hydraulics in outdoor open high density microalgal (Chlorella sp.) photobioreactorsoperated in a Middle and Southern European climate. *J Appl Phycol*. 2006;18:811–826.

34. Richmond A, Cheng-Wu Z. Optimization of a flat plate glass reactor for mass production of Nannochloropsis sp. outdoors. *J Biotechnol*. 2001;85:259–269.
35. Cornet JF, Dussap CG, Gros JB. Kinetics and energetics of photosynthetic micro-organisms in photobioreactors: application to Spirulina growth. *Adv Biochem Eng Biotechnol*. 1998;59:155–224.
36. Pottier L, Pruvost J, Deremetz J, Cornet JF, Legrand J, Dussap CG. A fully predictive model for one-dimensional light attenuation by Chlamydomonas reinhardtii in a torus reactor. *Biotechnol Bioeng*. 2005;91:569–582.
37. Loubiere K, Olivo E, Bougaran G, Pruvost J, Robert R, Legrand J. A new photobioreactor for continuous microalgal production in hatcheries based on external-loop airlift and swirling flow. *Biotechnol Bioeng*. 2009;102:132–147.
38. Sierra E, Acien FG, Fernandez JM, Garcia JL, Gonzales C, Molina E. Characterization of a flat plate photobioreactor for the production of microalgae. *Chem Eng J*. 2008;138:136–147.
39. Perez R, Seals R, Ineichen P, Stewart R, Menicucci D. A new simplified version of the Perez diffuse irradiance model for tilted surfaces. *Sol Energy*. 1987;29:221–231.
40. Duffie JA, Beckman WA. *Solar Engineering of Thermal Processes*. 3rd ed. New York: Wiley, 2006.
41. Cornet JF, Dussap CG, Gros JB. A simplified monodimensional approach for modeling coupling between radiant light transfer and growth kinetics in photobioreactors. *Chem Eng Sci*. 1995;50:1489–1500.
42. Pruvost J, Cornet JF, Legrand J. Hydrodynamics influence on light conversion in photobioreactors: an energetically consistent analysis. *Chem Eng Sci*. 2008;63:3679–3694.
43. Cornet JF, Dussap CG, Cluzel P, Dubertret G. A structured model for simulation of cultures of the cyanobacterium Spirulina platensis in photobioreactors. 1. Coupling between light transfer and growth kinetics. *Biotechnol Bioeng*. 1992;40:817–825.
44. Cornet J-F. Procédés limités par le transfert de rayonnement en milieu hétérogène. Etude des couplages cinétiques et énergétiques dans les photobioréacteurs par une approche thermodynamique [Habilitation à Diriger des Recherches]. Université Blaise Pascal - Clermont-Ferrand, n° d'ordre 236; 2007.
45. Eriksen NT, Geest T, Iversen JJ. Phototrophic growth in the lumostat: a photo-bioreactor with on-line optimization of light intensity. *J Appl Phycol*. 1996;8:345–352.
46. Vonshak A. *Spirulina platensis (Arthrospira): Physiology, Cell Biology and Biotechnology*. London, UK: Taylor & Francis, 1997.
47. Farges B, Laroche C, Cornet J-F, Dussap C-G. Spectral kinetic modeling and long-term behavior assessment of *Arthrospira platensis* growth in photobioreactor under red (620 nm) light illumination. *Biotechnol Prog*. 2009;25:151–162.
48. Gonzalez de la Vara L, Gomez-Lojero C. Participation of plastoquinone, cytochrome c553 and ferredoxin-NADP+ oxido reductase in both photosynthesis and respiration in Spirulina maxima. *Photosynth Res*. 1986;8:65–78.
49. Cornet JF. Etude cinétique et énergétique d'un photobioréacteur. Université Paris 11 - Orsay, n° d'ordre 1989; 1992.
50. Cornet JF, Dussap CG, Leclercq JJ. *Simulation, design and model based predictive control of photobioreactors*. In: Thonart P, Hofman M, editors. *Focus on Biotechnology, Engineering and Manufacturing for Biotechnology*. Vol. 4. Dordrecht: Kluwer Academic Publishers, 2001:227–238.
51. Kumar S, Felske J. Radiative transport in a planar medium exposed to azimuthally unsymetric incident radiation. *J Quant Spectrosc Radiat Transfer*. 1986;35:187–212.

Appendix: Modeling of Radiative Light Transfer in Bulk Culture in Solar Conditions

Modeling radiant light energy transport inside Cartesian geometry photoreactors[17,18] or turbid water media with photosynthetic microorganisms in open ponds[11,18] has long been a subject of study. In general, this problem has been demonstrated to be azimuthally independent, although not possibly in some particular applications.[51] These very interesting pioneer studies have mainly focused on the degree of sophistication of the numerical procedures used to solve the radiative transfer equation (among them the two-flux method), correctly distinguishing, for the boundary conditions, between the directional collimated and the diffuse components of the solar radiation. Nevertheless, these authors mainly considered simple generic radiative properties for the scatterers (mineral catalysts or microorganisms), whereas we have clearly demonstrated[36,44] that quasi-exact properties are a crucial requirement for a confident radiation field description in a PBR. In this case, the two-flux method seems sufficiently accurate as a first approximation[11,36] to calculate the radiation field, thus allowing the kinetic and stoichiometric coupling formulation. This method also presents the major advantage of giving analytical solutions (saving calculation time as an elemental stage of a complex dynamic model) for any considered boundary conditions, such as directional-collimated and diffuse-isotropic conditions generally encountered in incident solar radiation modeling.

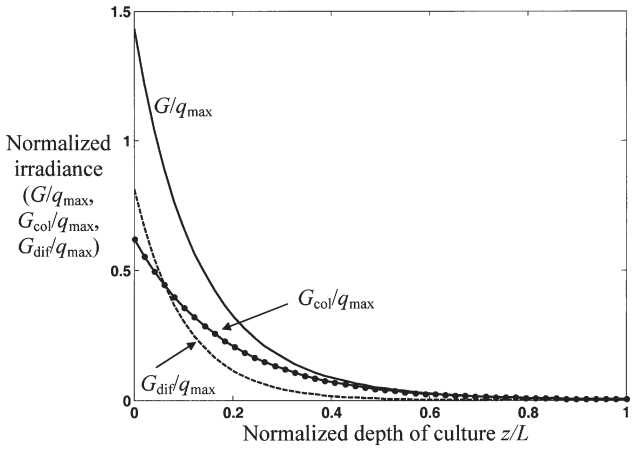

Figure A1. Examples of irradiance field in bulk culture for averaged summer day at noon.

Two examples of irradiance profiles are given in Figures A1 and A2. Each one derives from the simulations conducted in our work and were chosen to illustrate the specific radiative transfer conditions as a result of solar conditions

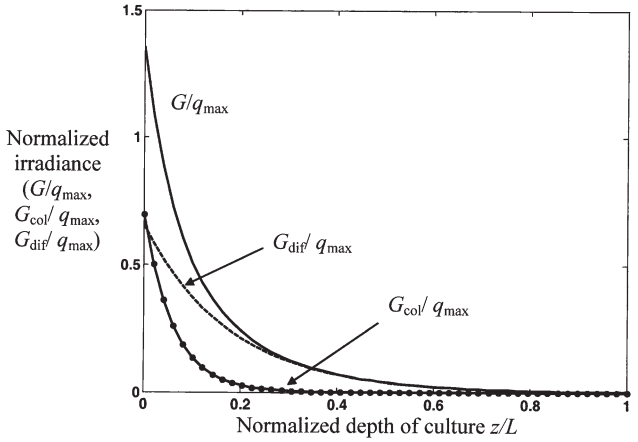

Figure A2. Examples of irradiance field in bulk culture for averaged winter day just before sunset.

Table A1. Investigation of Various Modeling Assumptions in the Radiative Transfer Calculation on Resulting Productivity (See Text for Details)

Areal Productivity (10^3 kg m^{-2} d^{-1})	Maximal Productivity	Assumption 1 (Normal Incidence)	Assumption 2 (All Radiation q Collimated)	Assumption 3 (Normal Incidence and All Radiation q Collimated)
Summer day, $\beta = 0°$	10	11.7	11.4	13.6
Winter day, $\beta = 0°$	2.8	3.4	2.1	4.1
Winter day, $\beta = 45°$	4.7	5.1	5.1	5.9

(both are for the horizontal inclination). Figure A1 represents the irradiance field obtained for the typical summer day at noon (12:00 h). As described in the text, this corresponds to the maximum of irradiation (total radiation $q = 1273$ μmol m^{-2} s^{-1} with direct radiation $q_{//} = 737$ μmol m^{-2} s^{-1}, diffuse radiation $q_{\cap} = 536$ μmol m^{-2} s^{-1}, and an incidence angle $\theta = 26°$). Figure A2 is for the typical winter day just before sunset ($t = 15{:}00$ h). A high incidence angle is observed with a significant part of diffuse radiation ($q = 130$ μmol m^{-2} s^{-1}, $q_{//} = 35$ μmol m^{-2} s^{-1} and $q_{\cap} = 95$ μmol m^{-2} s^{-1}, and $\theta = 80°$).

Those two examples show light attenuation inside the bulk culture. Corresponding light fraction $\gamma > 1$ (kinetic regime) and $\gamma = 0.9$ (full light absorption) were obtained for the summer (Figure A1) and winter (Figure A2) cases, respectively. These two examples also illustrate the respective contributions of direct and diffuse parts to the total irradiance field as defined by the sum of collimated and diffuse contributions. In all cases, none of the radiation component can be neglected, even for these two cases that emphasized one or the other of the radiation components (direct for summer and diffuse for winter). For the summer case, due to a low incident angle, beam radiation penetrates deeply inside the bulk culture. Because of its noncollimated nature, diffuse radiation (not sensitive to the incident angle) attenuates more rapidly. For the winter case, the main contribution comes from the diffuse component. This is explained here by the high incidence angle, which greatly reduces the penetration of the direct component of the radiation.

To emphasize the relevance of considering incidence angle and direct/diffuse distribution in the solar PBR model, simulations were conducted assuming different simplifications in the radiative transfer calculation. First, the effect of the incident angle was neglected, and a constant value $\theta = 0$ was applied in Eq. 2 (Assumption 1). Second, the direct and diffuse parts of solar radiation were not considered separately in the calculation, all radiation being assumed to be only collimated, with angle θ (Assumption 2). This was obtained by replacing $q_{//}$ (direct radiation) by q (sum of direct and diffuse radiations) in Eq. 2 and by ignoring the calculation of Eq. 3 (diffuse component). Third, as the simplest case of radiative transfer representation, the two previous assumptions were combined, and all the radiations were taken as being only collimated but with no effect of incident angle in the radiative transfer calculation (Assumption 3). The results are given in Table A1 with those calculated in this work for comparison (with time-varying incidence angle and a distinction between beam and diffuse components in solar radiation). As expected, the different assumptions influence productivity prediction. Except for the winter day with $\beta = 0°$ (see below), an overestimation was obtained. The assumption of normal incidence (Assumption 1) resulted in an increase in the light flux penetrating the PBR ($\cos\theta = 1$ in all calculations). In the same way, because diffuse radiation attenuated more rapidly in the culture medium, considering all the radiations to be only collimated (Assumption 2) tended also to increase the resulting productivity. In the studied case, both assumptions led to an overestimation of 10–20%, depending on the irradiation conditions. When the two assumptions were combined (the simplest case of radiative transfer representation), an overestimation of up to 50% was obtained. This emphasizes the relevance of an accurate consideration of the incident angle and direct/diffuse distribution in the radiative transfer modeling. As stated above, the only case where an overestimation was not obtained was for the winter day with $\beta = 0°$ and Assumption 2. An underestimation of 25% was then obtained. This is fully explained here by the special conditions of illumination obtained with a high incidence angle and with intercepted light composed mainly of diffuse radiation (as described). In Assumption 2, all intercepted radiations including diffuse radiation were considered as collimated radiation. However, the high incidence angle in this case caused beam radiation penetration to be greatly reduced. Because diffuse radiation formed the most significant part of the light intercepted here, this resulted in a reduction of the predicted productivity compared with the case where diffuse radiation (not influenced by the incident angle) was accurately considered. Neglecting incidence angle effect (as in Assumptions 1 and 3) prevented this effect (efficient penetration of collimated radiation), and productivity was then overestimated. This last example illustrates that both incident angle and direct/diffuse radiation can have a complex influence on the resulting radiative transfer modeling inside the bulk culture, depending on the radiation conditions investigated. An accurate representation of both effects is thus necessary to take accurately into account their respective importance for PBR productivity.

Manuscript received Mar. 3, 2010, and revision received July 22, 2010.